An investigation into the effectiveness of various advanced CT methods in the reduction of metal artefacts

Matthew Dixon
(MatthewDixon@nhs.net)

Robert Loader

With thanks to:
Professor Carl Roobottom
Dr Philip Coates
Dr Vincent Vardhanabhuti
Plymouth Mechanical Workshop

1. Assumptions made in forming a CT image
2. Artefacts arising from these assumptions
3. Ways of reducing or eliminating these assumptions (advanced CT methods)
4. Experimental design
5. Results
6. Discussion and future work

1. Assumptions made in forming a CT image

- If we could directly derive the exact attenuating properties of our area of interest from our dataset then we would have a ‘perfect’ image

- It is the (necessary) assumptions that are made which lead to all misrepresentations of the true situation (artefacts)

1. Assumptions made in forming a CT image

Ideal situation

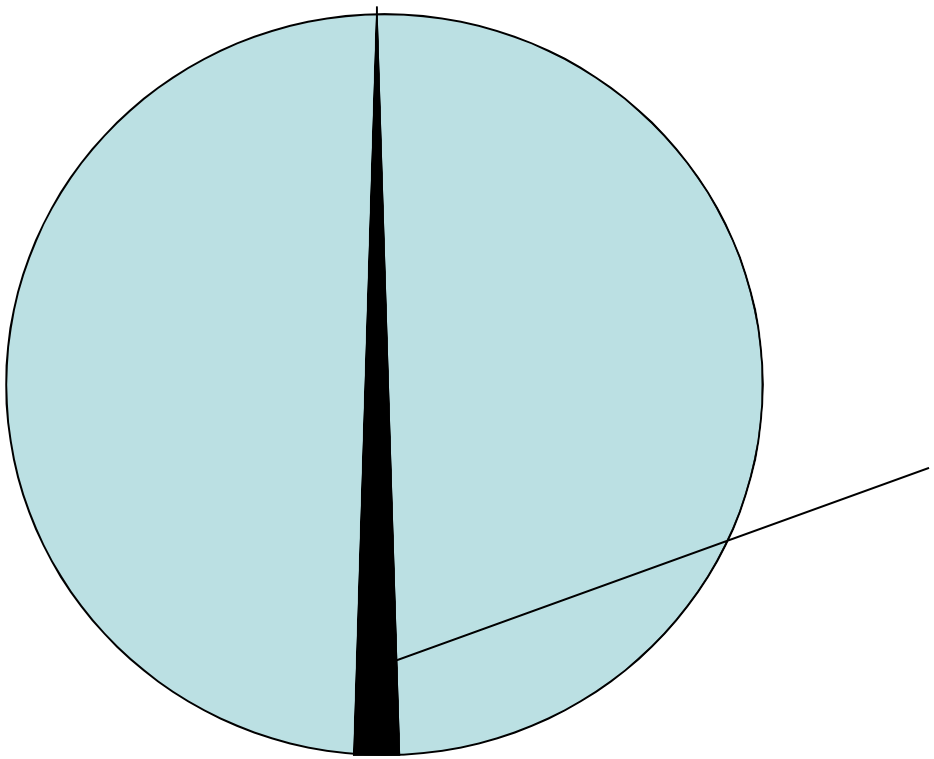

Energy independent, perfect beam with no variation in attenuation orthogonal to the beam

<u>Primary Assumptions</u>

-Point source and uniform orthogonal attenuation

-No Energy Dependence

-Perfect Source and Detector Statistics

1. Assumptions made in forming a CT image

Finite Beam

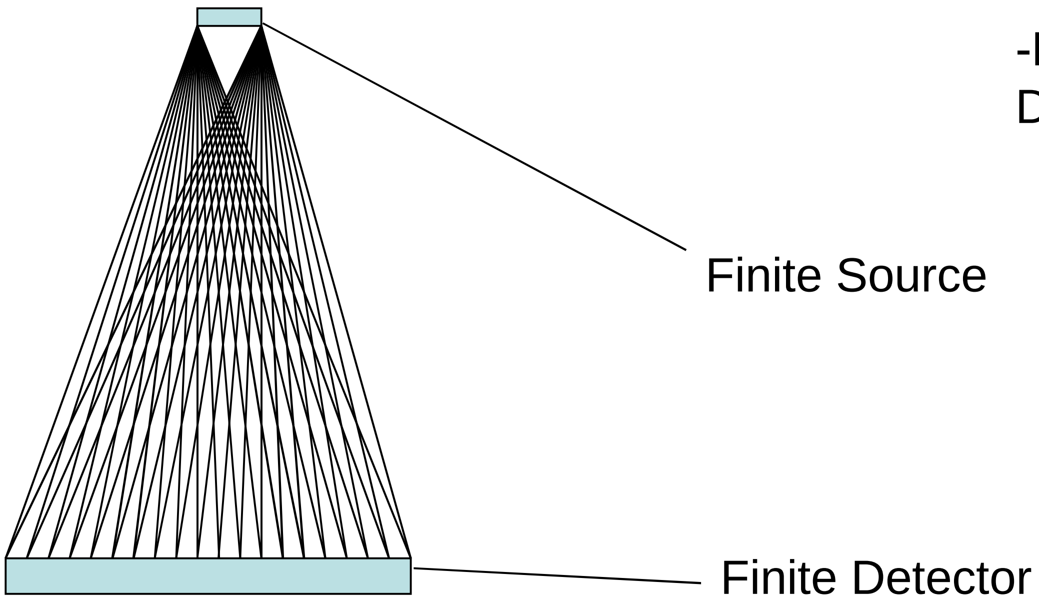

Primary Assumptions

-Point source and uniform orthogonal attenuation

-No Energy Dependence

-Perfect Source and Detector Statistics

1. Assumptions made in forming a CT image

Energy Dependence

Primary Assumptions

-Infinitesimal Line and detector

-No Energy Dependence

-Perfect Source and Detector Statistics

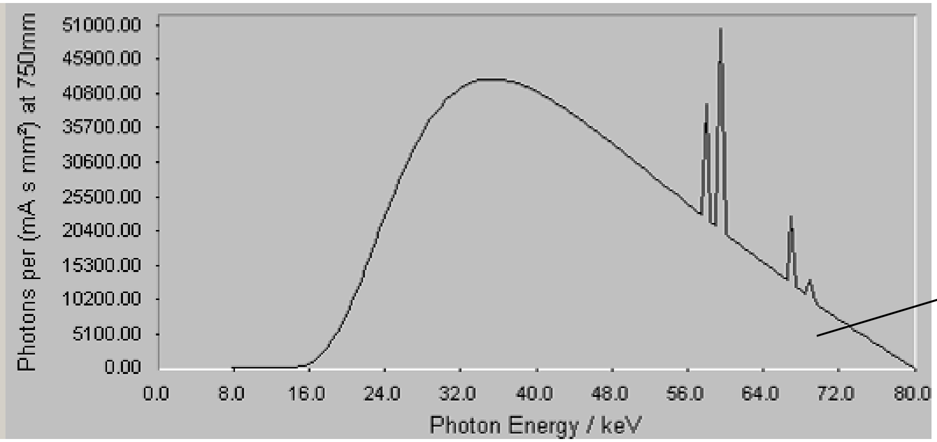

80kV spectrum with 2.5mm Al filter produced using Report 78 Spectrum Processor © IPEM 1997

Spectrum of energies, each attenuates differently

Statistics

The emission of X-Ray photons and the detection of these in the detector is considered to be governed by Poisson statistics

As the average source intensity is much greater than the average detector intensity it is detector statistics which are the most relevant

$$P(I_M, \overline{I_M}) = \frac{\overline{I_M}^{I_M} e^{-\overline{I_M}}}{I_M!}$$

Probability that the measured intensity is I_M given the average measured intensity $\overline{I}_M$

Primary Assumptions

-Point source and uniform orthogonal attenuation

-No Energy Dependence

-Perfect Source and Detector Statistics

Result

Every one of the mentioned assumptions leads to a certain type of artefact

Detector statistics – Noise and photon starvation

- General uncertainty in scan leads to random statistical fluctuations (noise)

- Where individual projections have passed through areas of high attenuation the uncertainty in the calculated attenuation becomes very high and leads to streaks emanating from the object

Energy Dependence – Beam hardening

- Low energy components are absorbed preferentially, especially in high Z materials where the photoelectric effect is dominant
- Low energy spectrum absorbed to a point where it can provide no contrast
- Reduction of contrast and measured attenuation in projections that pass through high Z, dense objects.

Finite beam – Partial volume effects

- Attenuation is a non-linear process (exponential)
- Measured intensities are averaged across the detector and therefore averaged over several beam paths

$$\ln\left(\frac{\bar{I}}{I_0}\right) \neq -\bar{\mu}x$$

- This means that in beams where the attenuation varies significantly, there could be a misrepresentation of the data.

Plymouth Hospitals NHS
NHS Trust

2. Artefacts arising from these assumptions

Beam starvation/Beam Hardening streaks caused by a pacemaker

Dual Energy - background

a	b	c
d	f	g
h	i	j

At energy E_0

→

A(E)	B(E)	C(E)
D(E)	F(E)	G(E)
H(E)	I(E)	J(E)

For any energy

Constants (attenuation coefficients)

Functions (coefficients and a base set)

Dual Energy - background

Photoelectric coefficient, this is the energy independent photoelectric coefficient unique to each material and density

Compton base, this is the Compton energy dependent function, it is independent of material

Klein Nishina

$$\mu(x,y;E) = a_p \mu_p + a_c \mu_c$$

Photoelectric base, this is the photoelectric energy dependent function, it is independent of material

$$\mu_p = \frac{1}{E^3}$$

Compton coefficient, this is the energy independent Compton coefficient unique to each material and density

Dual Energy - background

- Photoelectric and Compton terms replaced by Iodine and Water to allow calibration of the scanner (require knowledge of energy spectrum)

- Now have theoretically energy independent information allowing simulation of any energy

Dual energy - Application

As the energy dependence has been theoretically removed entirely there should be no beam hardening artefacts at all

Other effects on metal artefacts are not obvious.

Iterative techniques

ASIR (Adaptive Statistical Iterative Reconstruction) simulates system statistics by weighting the projections

VEO is a form of model based iterative reconstruction and models the finite source and detector.

HD scanning

- Greater number of projections by altering source position (focal spot)

- Potentially improved resolution

Specifically designed algorithms

Most of these use interpolative techniques in the sinogram, some use iterative techniques

All algorithms essentially use information from projections that do not pass through metal to correct ones that do

4. Experimental design

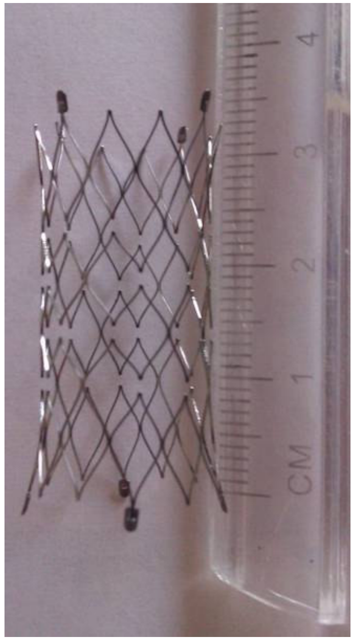

Method

- Scanned each metal object in turn in the phantom using iodine/water mixes to simulate different contrasts
- Scanned at 120kVp and 140kVp with HD mode on and off, and reconstructed with ASIR and VEO (not available for HD)
- Also scanned in dual energy mode and reconstructed at four different keVs

5. Results

Results

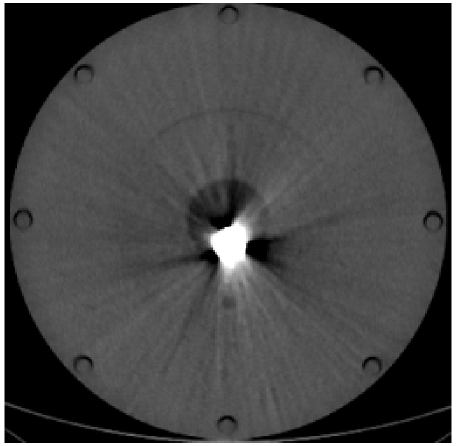

140keV GSI

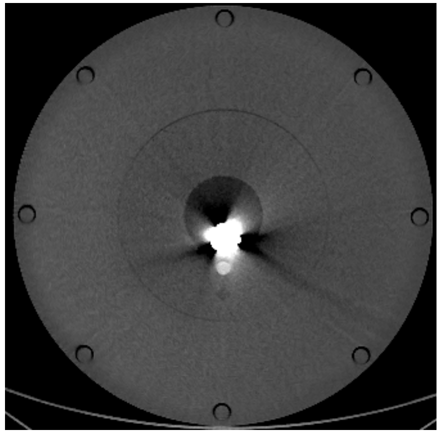

VEO 140kV

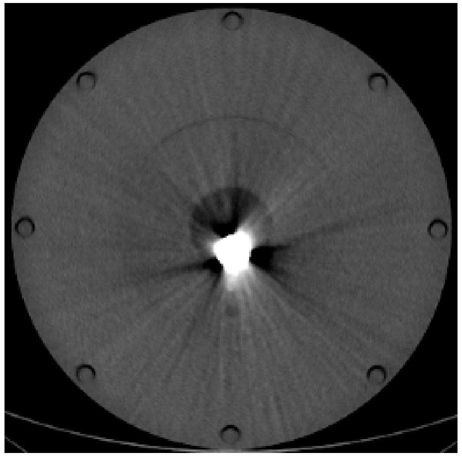

100keV GSI

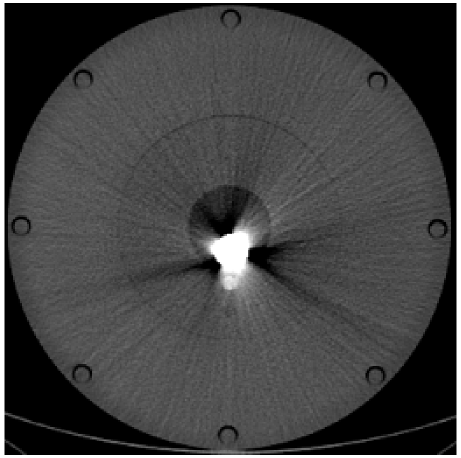

FBP 140kV

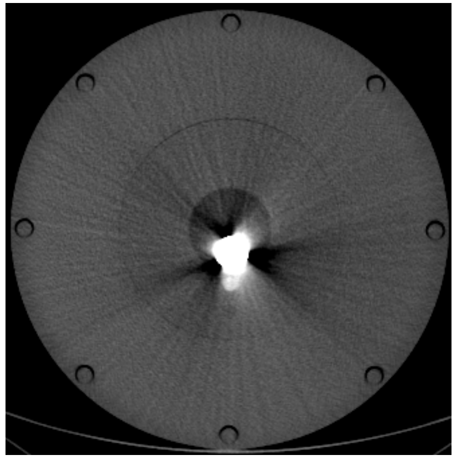

FBP HD 140kV

MARS

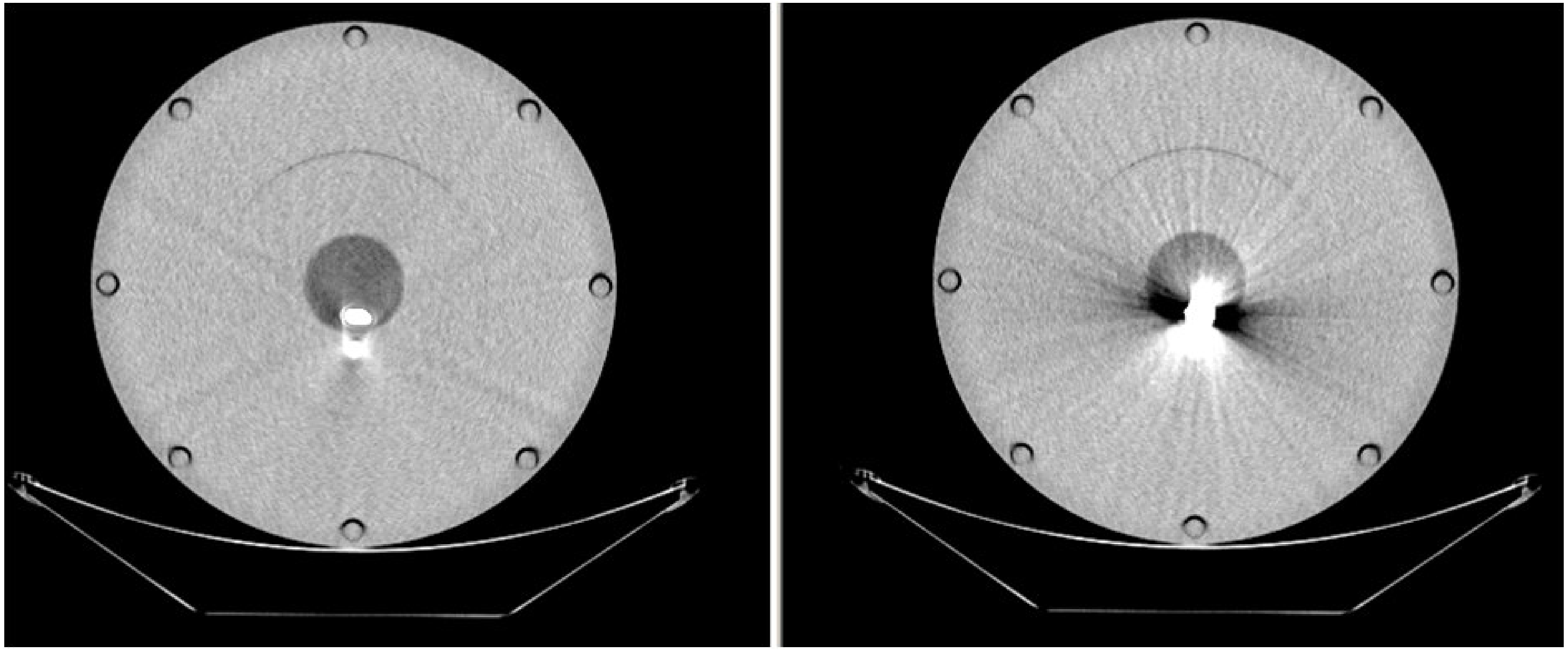

A 70keV reconstruction of a slice through a Hip Prosthesis with (left) and without (right) MARS

MARS

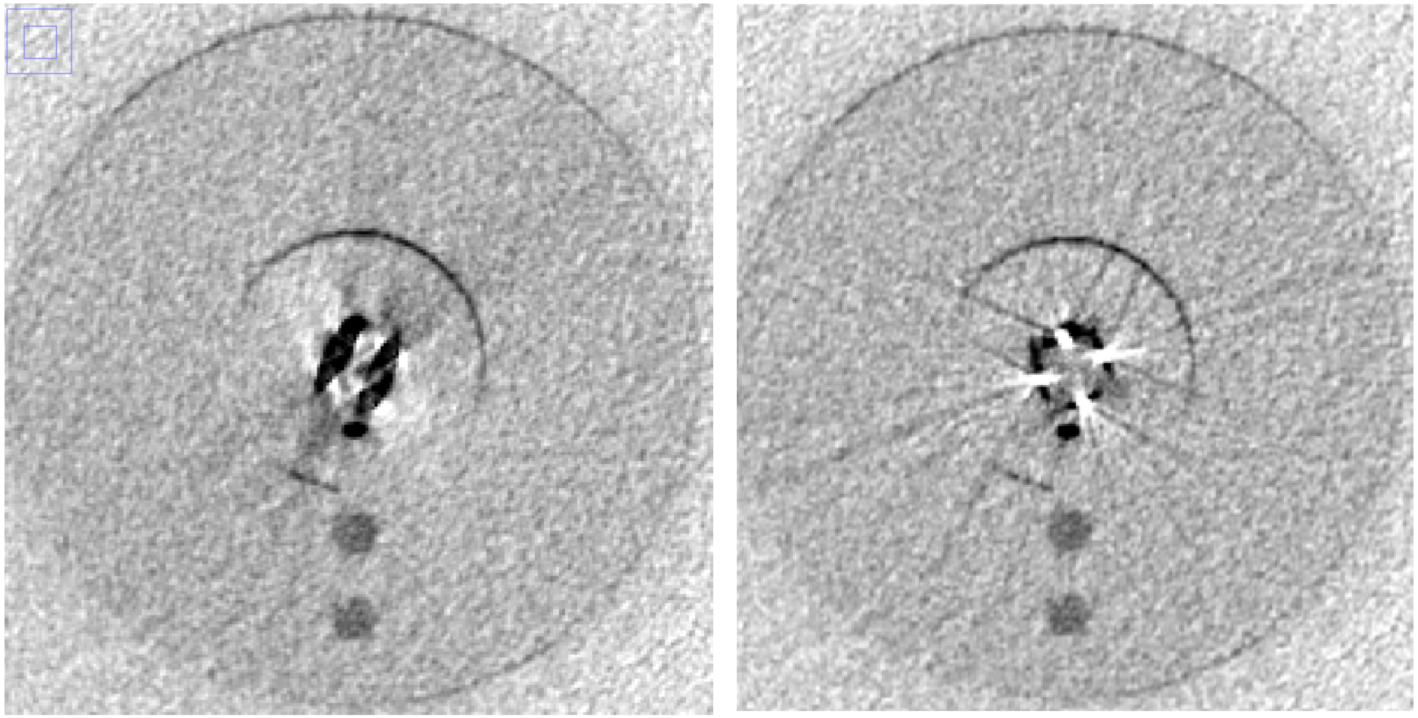

A 70keV reconstruction of a slice through a stent with (left) and without (right) MARS

Results – ROI analysis

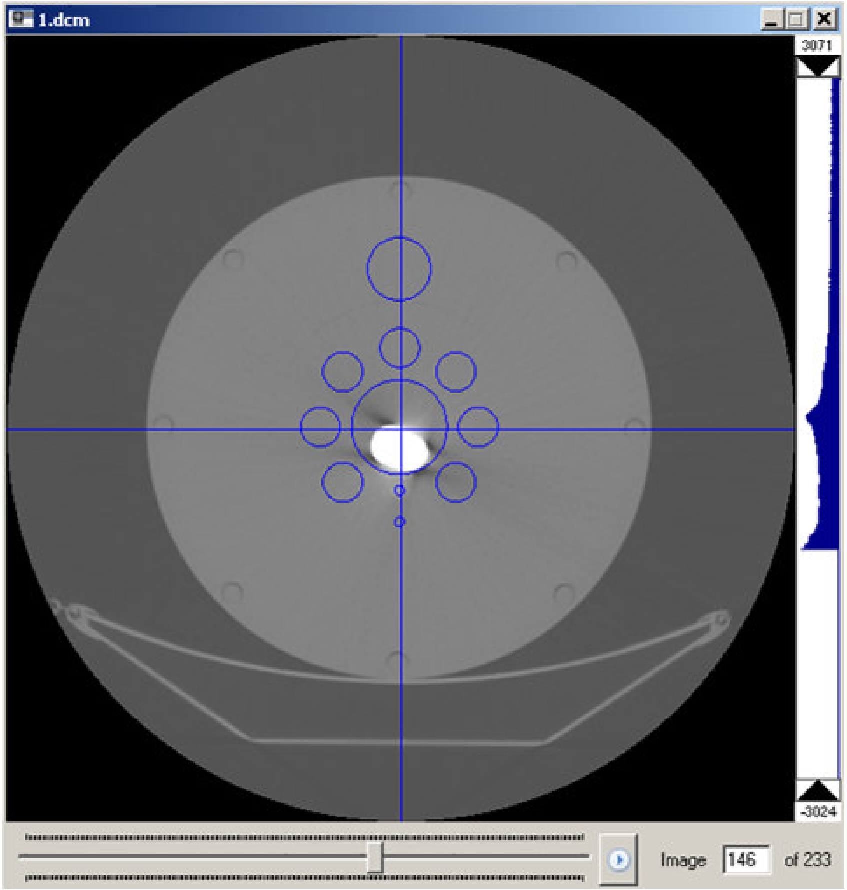

-Used IQ works to allow reproducible processing of many slices

-Took standard deviation between the means of the 7 region of interest

-Used contrast to noise ratio of two small holes to large top hole

5. Results

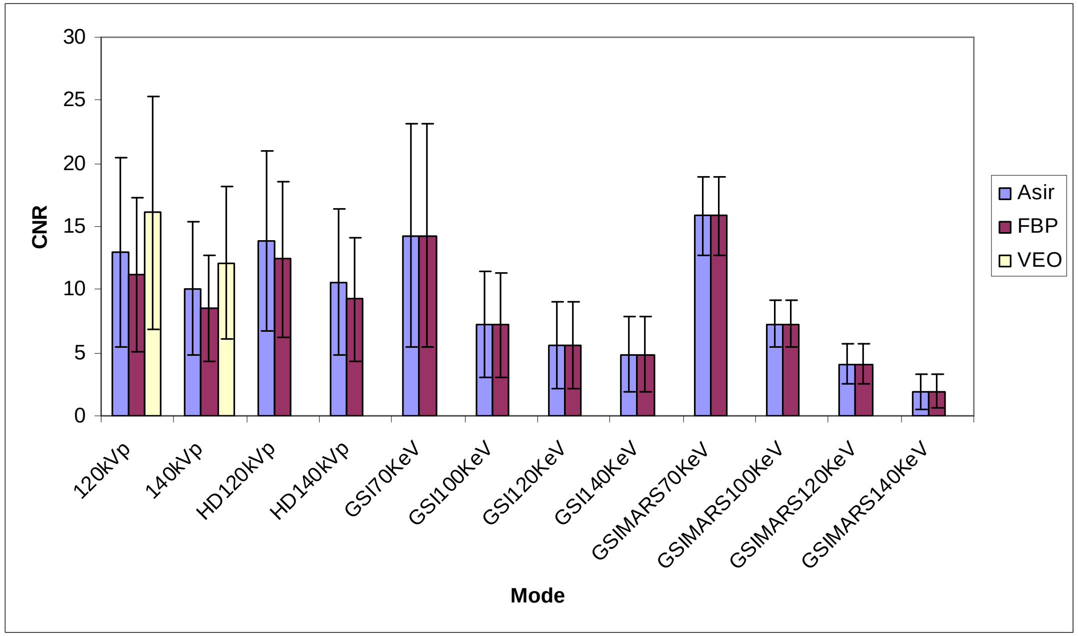

Prosthesis

The average contrast to noise ratio (CNR) of the middle insert (high contrast) across the various modalities. The uncertainty is represented by the standard deviation of the slices

The average contrast to noise ratio (CNR) of the outer insert (low contrast) across the various modalities. The uncertainty is represented by the standard deviation of the slices

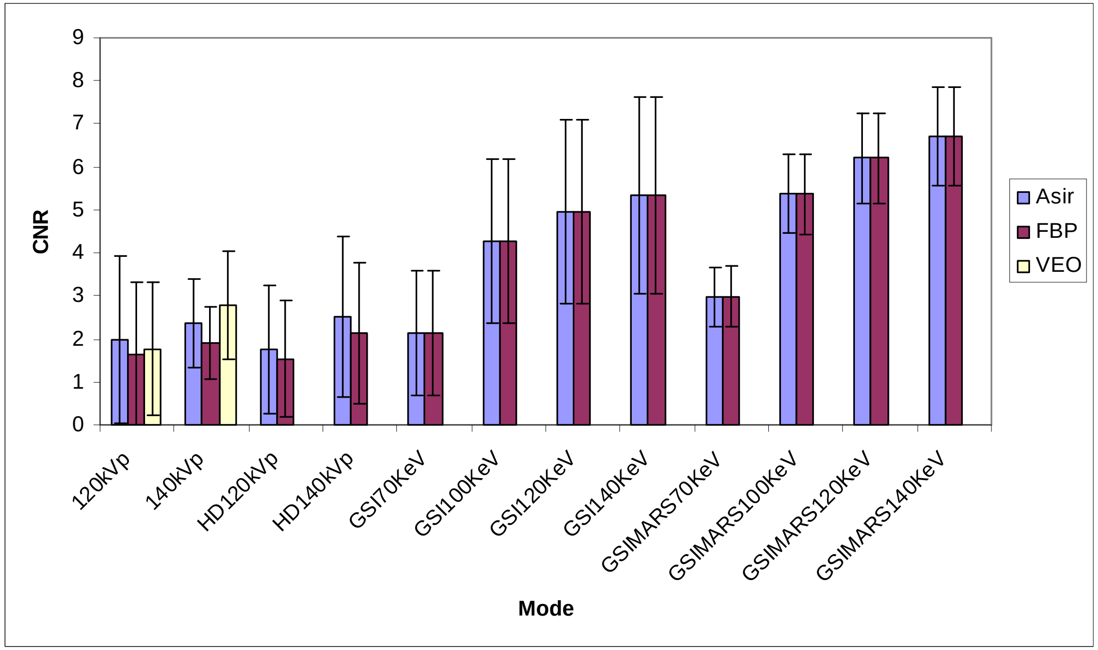

5. Results

Prosthesis

The average standard deviation between mean Hounsfield number in the Seven regions of interest, the uncertainty is represented by the standard deviation of the slices

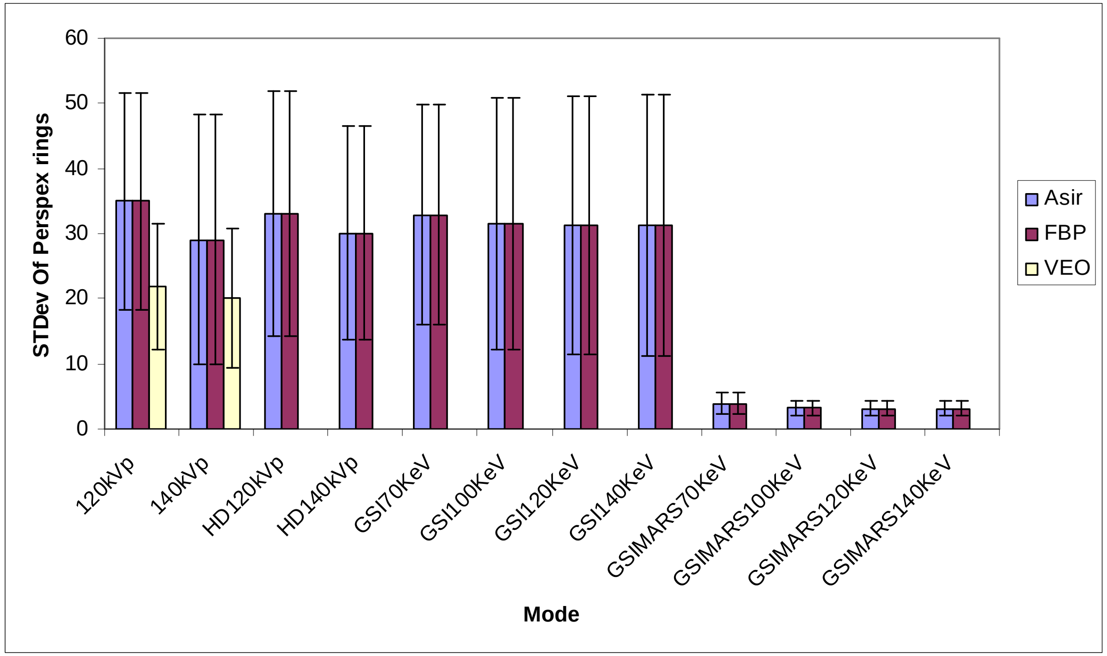

5. Results

Stent

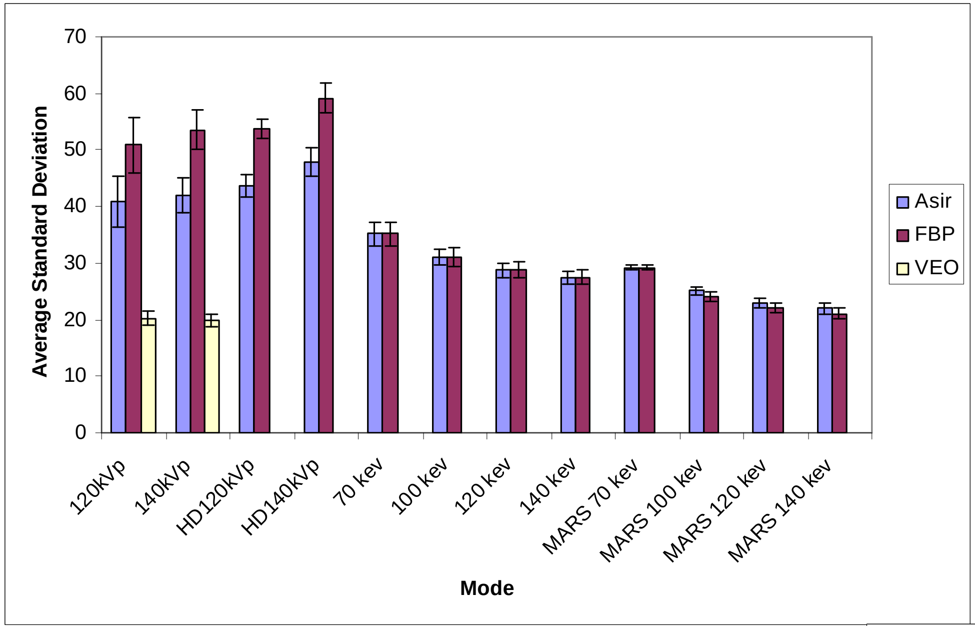

The average standard deviation across the seven regions of interest for the different modalities, the uncertainty is represented by the standard deviation of the slices

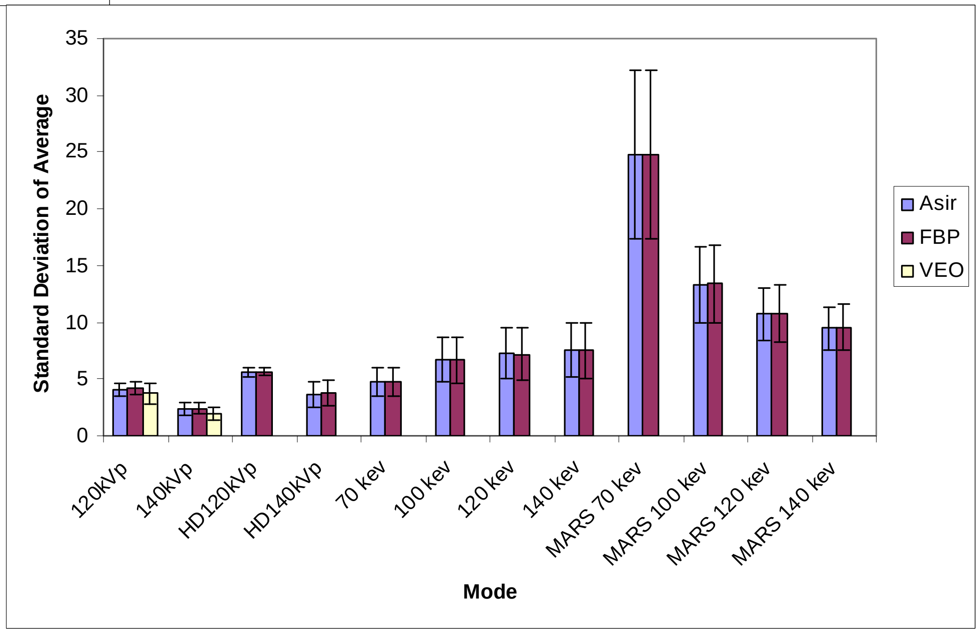

The average standard deviation between mean Hounsfield number in the Seven regions of interest, the uncertainty is represented by the standard deviation of the slices

5. Results

Coil

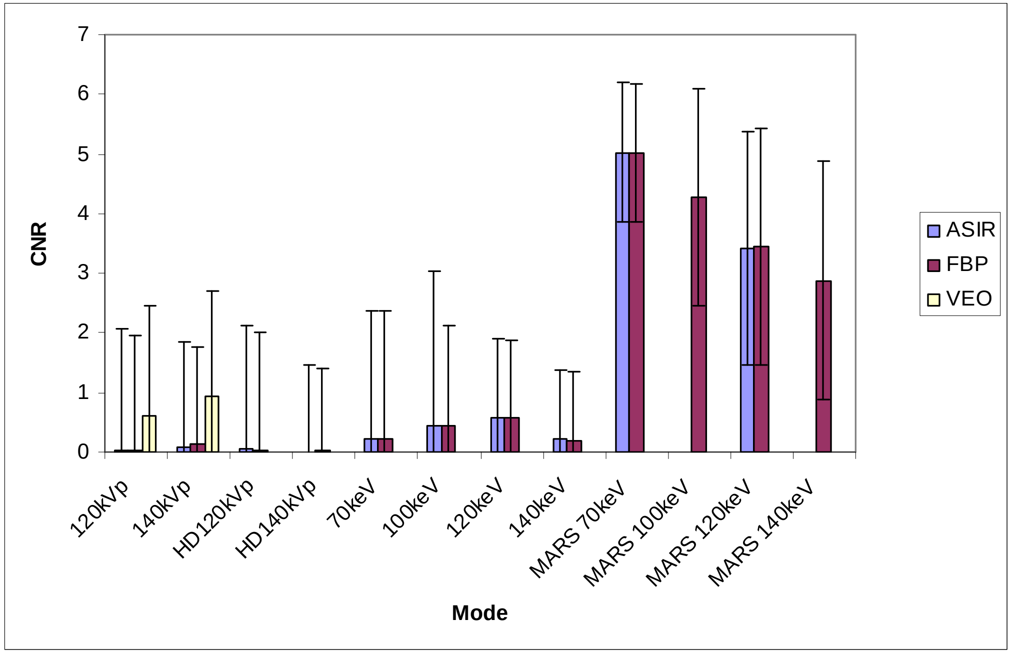

The average Contrast to Noise Ratio (CNR) of the contrast area as compared to background, the uncertainty is represented by the standard deviation of the slices

Discussion

- GSI with MARS appeared to be the most effective of those methodologies tested with VEO being the second
- GSI with MARS can cause unusual artefacts in rare situations
- The ability to see different contrasts is affected by choice of keV

Discussion

- With these in mind, GSI with MARS has potential for situations where metal objects would otherwise render the image undiagnostic
- It would be prudent to view the image at several different keV settings to ensure the full range of contrasts is represented
- It would be prudent to view the images both with and without MARS applied to check no unusual artefacts have been created
- If GSI is used consultants will need to adapt to the different kind of information available

Future Work

- An improved way to compare algorithms (ROI method crude)
- Compare to metal deletion algorithms that use one spectrum
- Evaluate other dual energy systems, particularly dual tube systems

Last page!

Thank you very much for listening, are there any questions?

Plymouth Hospitals NHS
NHS Trust

References

- The National Institute Of Standards (NIST), Physical Measurement Laboratory [Online], Available at http://physics.nist.gov/PhysRefData/Xcom/html/xcom1.html, [Accessed August 2012]
- Frequency split metal artefact reduction (FSMAR) in Computed topography, E. Meyer et al., **Medical Physics** 39 (4), April 2012
- Metal artefact reduction for CT: Development, implementation and clinical comparison of a generic and scanner specific technique, R.M.S Joemai et al., **Medical Physics** 39 (2), February 2012
- CT Metal artefact reduction method correcting for beam hardening and missing projections, J.M Verburg, J Seco, **Physics in Medicine and Biology** 57, 2803 – 2818, 2012
- Development, implementation and evaluation of a dedicated metal artefact reduction method for interventional flat-detector CT, D Prell et al., **The British Journal of Radiology** 83, 1052-1062, 2010
- Iterative correction of beam hardening artifacts in CT, G Van Gompel et al., **Medical Physics** 38 (7), S36 – S49, July 2011
- Iterative deblurring for CT metal artefact reduction, G. Wang et al., **IEEE transactions on medical imaging** 15 (5), October 1996
- B. De Man et al. Metal Streak Artifacts in X-Ray Computed Tomography: A simulation study, **IEEE**, 1860 – 1865, 1999
- P Joseph, R Spital, The exponential edge-gradient effect in x-ray computed tomography, **Physics in Medicine and Biology** 26 (3), 473 - 487, 1981
- H Xue et al., Metal artifact reduction in Dual Energy CT by Sinogram Segmentation Based on Active Contour Model and TV Inpainting, **IEEE Nuclear Science Symposium Conference record**, 904 – 908
- P Sukovic and N Clinthorne, Penalized, weighted Least squares Image reconstruction for dual energy X-Ray transmission tomography, **IEEE transactions on medical imaging,** 19 (11), November 2000
- A framework for spectral artefact correction in CT, J.P.StoneStrom et al., **IEEE transactions on biomedical imaging,** 28 (2) 128-141, February 1981
- Metal artefact reduction in gemstone spectral imaging dual-energy CT with and without metal artefact reduction software, Y.H.Lee et al., **European Radiology**, Volume 22 6 (2012), 1331-1340
- Comparison of four dual energy image decomposition methods, K.S.Chuang, H.K.Huang, **Physics in Medicine and Biology** 33 (1988) No 4, 455-466
- **Journal of the ICRU,** report 81, Quantitative Aspects of Bone Densitometry
- Metal artifact reduction by dual energy computed tomography using monoenergetic extrapolation, F.Bamberg et al., **European Radiology** 21 (7) , 1424 - 1429, 2011
- Improved Image Quality in Dual-Energy Abdominal CT: Comparison of Iterative Reconstruction in Image Space and Filtered Back Projection Reconstruction, W.Rui et al., **American journal of Roentgenology** 199 (2), August 2012
- IQ Works V 0.7, EdMcDonagh et al. [Online], Available at http://wiki.iqworks.org/Main [Accessed August 2012]
- Leeds Test Objects Medical Imaging Phantoms, Leeds Test Objects [Online], Available at http://www.leedstestobjects.com/ [Accessed August 2012]
- CTDI phantom, ImpactScan